Chronicles of Biomedical Sciences
ISSN:3065-923X
Homepage: https://cbsciences.us/index.php/cbs

In-silico Analysis of Potential Phytochemicals against VP39 Methyltransferase of Monkeypox virus

Aiman Aftab[1], Rana Muhammad Mateen[1], Muhammad Sohail Afzal[1]

[1]University of Management and Technology, Lahore, Pakistan.

ORIGINAL ARTICLE

Received on: April 27, 2025.

Accepted on: May 14, 2025.

Published on: May 15, 2025.

Keywords: Density functional theory; In-silico study; Molecular docking; Monkeypox virus; VP39 Methyltransferase.

Corresponding author: Rana Muhammad Mateen
mateenibb@yahoo.com

ABSTRACT

Background: Monkeypox virus (MPXV), a zoonotic orthopoxvirus, has emerged as a global health concern, especially after the 2022 outbreak. Despite the rising prevalence, no drug has been specifically designed to treat MPXV. The VP39 methyltransferase (MTase) plays a vital role in mRNA capping, assisting the virus in immune evasion and replication, making it a promising antiviral target.
Objectives: This study aimed to identify natural phytochemical inhibitors against VP39 MTase of MPXV using computational drug discovery techniques, including molecular docking and density functional theory (DFT).
Methods: The crystal structure of VP39 MTase (PDB ID: 8cer) was obtained and validated using ERRAT, Verify3D, and PROCHECK. A total of 17,967 phytochemicals from the IMPPAT 2.0 database were screened based on ADMET properties and drug-likeness rules (Lipinski's and Veber's). Ninety-six compounds passed these filters and were docked using AutoDock Vina. The top ten ligands with the lowest binding energies were selected for further analysis, including interaction profiling and DFT evaluation to determine their chemical reactivity.
Results: The VP39 MTase structure was verified to be of high quality, with 93.5% of residues in the most favored regions. Among the 96 screened compounds, Hispidin (PubChem ID: 54685921) showed the lowest binding energy (-7.6 kcal/mol). Interaction analysis revealed multiple favorable interactions with active site residues. DFT analysis demonstrated a low HOMO-LUMO energy gap (ΔE = 0.12726 eV), suggesting high reactivity and potential as an effective inhibitor.
Conclusion: Hispidin emerged as a potent phytochemical candidate against VP39 MTase, showing strong binding affinity and favorable electronic properties. These findings provide a promising basis for further in vitro, in vivo, and molecular dynamics studies to develop novel anti-MPXV therapies

Citation: Aftab A, Mateen RM, Afzal MS. In-silico analysis of potential phytochemicals against VP39 methyltransferase of Monkeypox virus. Chron Biomed Sci. 2025;2(2):51. Available from: https://cbsciences.us/index.php/cbs/article/view/51.

Introduction

Monkeypox (Mpox) is caused by a double-stranded DNA enveloped virus called monkeypox virus (MPXV). It is a zoonotic viral disease with symptoms similar to small pox that can be transmitted from animal to humans or human to human, an orthopoxvirus (OPXV). MPXV specifically belongs to Chrodopoxvirinae sub family and Poxviridae family member [1]. The original source of Mpox are not monkeys because the first case was observed in macaque monkeys and that's why the virus was named as MPXV. Small mammals and rodents have been suspected as a source of MPXV, while the exact origin remains uncertain [2]. In 1958, when monkeys being transported from Singapore to Denmark due to illness with skin disease, MPXV was first time isolated in it. In the Democratic Republic of the Congo in 1970, the first human case in a child was diagnosed [3]. Recently, growing number of

Mpox has highlighted the global concern beyond its endemic regions. In laboratory monkeys in 1958, Mpox was initially detected and later recognized as human pathogen in 1970s [4]. Following the recent COVID-19 pandemic, 2022 outbreak of MPXV has initially sparked the concern about possibility of another emerging pandemic. In 2022, the largest outbreak of MPXV emerged, surpassing 57,000 cases across 103 countries with Europe, Brazil and US enduring the highest infection rate. In response to increasing MPXV outbreak, the World Health Organization (WHO) announced it a Public Health Emergency of International Concern on July 23, 2022 [5]. MPXV is primarily considered endemic to Central and West African countries, although has been reported in various regions across the world in recent years [2].

Through close contact with body fluids or bite from an infected animal, MPXV is usually transmitted. Close contact with infectious skin lesion spreads MPXV until scabs shed with possible transmission with large respiratory droplets from coughing and sneezing [6]. MPXV replicates at the entry side after entering the host and spread through lymphatic system causing systematic infection [7]. There is also a risk pf MPXV being transmitted from mother to fetus across the placenta (leading to congenital mpox) [8].

In the present mpox, the primary route of infection has largely spread through sexual transmission. The initial symptoms include headache, fever, swollen lymph nodes, muscle aches, backache and exhaustion. Rash emerges within 1-3 days after fever begins but sometimes takes longer. The onset of rash generally begins to appear on face and afterward transmit to other body parts. It has been reported that, the Mpox disease has been associated to cause death in up-to 10% of cases in the most severe outbreaks in Africa [9].

Due to absence of definite drug for Mpox treatment, CDC (centers for disease control and prevention) recommended using the small pox drugs such as Cidofovir, tecovirimat and vaccines that are effective for recent outbreak of MPXV that inhibit the viral DNA polymerase [10]. The only vaccine approved by FDA on 9 August 2022 is JYNNEOS and is used only for emergency to protect against MPXV. For orthopoxviruses, tecovirimat is more specific. Tecovirimat is administered to treat Mpox patient with severe symptoms and prevent the formation of enveloped virus. During 2022 outbreak, it was then approved by FDA, although the clinical results are yet uncertain [11][12]. Currently, no drug has been specifically designed against MPXV that emphasized the urgent need of developing effective antiviral treatments [12].

The antiviral drugs and current vaccines are insufficient because of rapidly increasing MPXV outbreak [13]. Due to high cost and ethical standards, direct testing on live beings has become considerably more difficult. As a result, in-silico techniques have shown effectiveness and evolved into powerful tool in disease research and drug discovery [12][14]. Modern techniques of drug designing such as drug repurposing may help to provide the more instant solutions [15].

MPXV, enclosed by lipoprotein membrane, is a double-helix DNA virus of the genus orthopoxvirus. All the necessary proteins are in poxvirus genome for transcription, assembly and replication and exit. Although it depends on host's ribosome to translate the mRNA [16]. An understanding of molecular structure of target virus is necessary for the development of drug. MPXV genome contain 197kb long that encode around 200 protein [10]. Being a DNA virus, MPXV entirely complete its life cycle and replicates within cytoplasm of infected cells [17]. MPXV starts uncoating and producing early genes during DNA replication after attachment with host cell [18].

Mpox possesses an RNA processing unit with an RNA capping machinery and replicates in the cytoplasm. For RNA capping in MPXV, the protein VP39 methyltransferase (MTase) (PDB ID:8cer) is crucial [19]. VP39 enzyme in MPXV, a key 2'-O-RNA methyltransferase, essential for RNA replication and transcription [20]. Studies confirms that VP39 MTase is a promising drug target due to its role in replication mechanism [19][21].

Through the process of methylation, this enzyme facilitates RNA synthesis in viruses and acting as a protective shield for viral RNA against host attacks [20][22]. VP39 MTase play vital role in translation and immune evasion through modifying cap structure of viral mRNA and ultimately enables successful infection and replication within host cells. For the development of efficient antiviral drugs, the current study suggests VP39 MTase as a potential target for MPXV inhibition [23][24].

To create a structural model VP39 MTase (PDB ID:8cer) for drug discovery, we resolved its crystal structure at 2.60Å and 297 amino acids reported through x-ray crystallization. It serves as an attractive anti-MPXV drug target due to the importance of VP39 MTase in viral replication and immune evasion. We used phytochemical library (IMMPAT) [25] containing 17967 compounds that were screened out on the basis of ADMET criteria. After careful evaluation, the selected ligands were further screened to identify potential inhibitor against protein VP39 MTase (PDB ID:8cer) of MPXV through molecular docking, Density functional theory (DFT) and MD Simulation. Using computational analysis, our study aimed to identify a natural inhibitor for this enzyme [24].

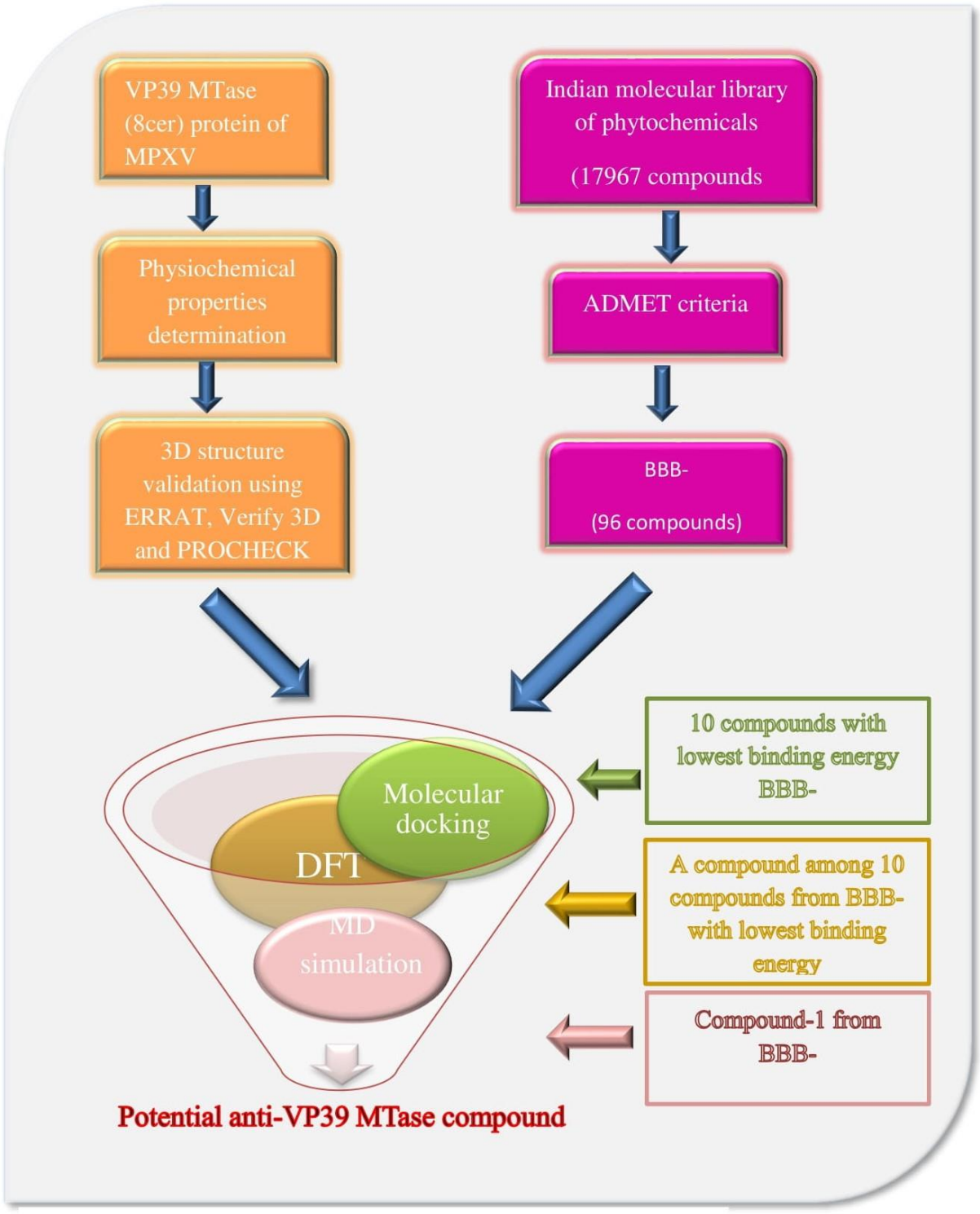

Figure 1. Illustration of the processes used in the current study

Methods

Illustration of the processes used in the study is shown in Figure 1.

3D structure selection

Only protein structures obtained through X-ray crystallography were utilized for analysis to ensure high resolution structural data. From RCSB-PDB, crystal structure of targeted protein VP39 MTase (PDB ID:8cer) of MPXV (Figure 2) has 297 amino acids and 2.60Å resolution was selected and retrieved. Structure was chosen on the basis of structural coverage and fine experimental resolution. Based on its excellent resolution (2.60Å) and the presence of key binding sequence (amino acids 1-297) that interacts with host receptors, from Protein Data Bank PDB ID:8cer was selected. Selecting an X-ray crystallography-based structure ensures the identification of binding pockets and overall protein confirmations [25].

Structure validation

Various quality assessment tools were employed to evaluate the accuracy of three-dimensional structure of protein VP39 MTase (PDB ID:8cer). From structure analysis and verification server version 6 (SAVES v6.0), three tools were used to verify the quality of VP39 MTase (8cer). ERRAT server [26] was used for analyzing protein's three-dimensional framework efficiency. To verify the compatibility of amino acid residues in the atomic model (3D) and to compare the results with existing structures, verify 3D server was utilized [27]. For quality assessment of existing and modeled structures, PROCHECK [28] server was used [29]. To assess the proteins quality, verification process was conducted. Results validating that it was of high standard protein [30][31][32].

Analysis of physiochemical properties

ExPASY PortParam tool was used to examine the physiochemical characteristics of target VP39 MTase (8cer) including Aliphatic index, log p, molecular weight, GRAVY score, predicted half-life, the amount of positively and negatively charged residues, atomic formula and the number of amino acid residues. Relative abundance of aliphatic side chain amino acid residues was indicated by aliphatic index. GRAVY score provided insights into protein's stability and obtained by dividing the total hydropathy of amino acids in the protein sequence. Like the concentration of a substance in the body to diminish by half, the half-life estimated the time needed for a specific parameter. Isoelectric point (PI) providing insight into its classification whether it is acidic or basic and corresponds to PH where it carries no net charge [30].

Receptor preparation

The target protein VP39 MTase (8cer) was purified by removing entities other than proteins like heteroatoms, water molecules and ligands with the help of BIOVIA Discovery Studio Visualizer [33]. Only chain A containing 297 amino acid residues of 8cer was retained. Protein was saved in the PDB format once purified. Then further proceeded for receptor preparation by using Auto Dock 1.5.7v tools [34][35]. Gasteiger charges and Polar hydrogen atoms were incorporated with the help of Auto Dock 1.5.7v tools and then converted PDB into PDBQT format.

Binding site prediction and grid box generation

Literature review was conducted to identify active site of protein VP39 MTase (8cer). For ligand binding site visualization, three online servers were also used named COACH [36], PrankWeb [37] and CASTp [38]. For analysis in these servers, protein structure was served as input in the PDB format. Their analysis shows the possible binding pockets in the protein VP39 MTase (8cer). COACH, meta server, was utilized for binding site prediction. Using TM-SITE and S-SITE approaches, to detect ligand-binding template from BioLiP protein function database using sequence and substructure profiling. This analysis uncovered potential binding pockets within a protein [12]. CASTp highlighted binding areas, active sites and analyzed interaction zones of amino acid along with their measured volumes and areas [30].

For docking the ligands against the active site of receptor, a grid was generated around the protein VP39 MTase (8cer). Auto Dock 1.5.7v tools was employed to create the grid on VP39 MTase active site residues. Active site residues of VP39 MTase (8cer) were Q37, G38, Q39, K41, L42, F285, D228 and E233 were used for receptor-grid generation. The grid box center was positioned at 10.676Å, 10.205Å and 45.918Å with the dimensions of 30 × 30 × 45 along the x, y and z coordinates respectively. The exhaustiveness parameter was set at 8 with a grid spacing of 1.0Å.

Ligands library

Indian Medicinal Plants, Phytochemistry and Therapeutics 2.0 (IMPPAT 2.0) [25] is an online library of phytochemicals. From this library, ligand library which contain 17967 phytochemicals was taken for further docking processes.

Screening of ligands library

After acquiring 17967 ligands from IMPPAT 2.0 [25], which were screened following ADMET properties as shown in Table 1. First applied Lipinski Rule of five (ROF)

to identify the drug likeliness of compounds [39]. Based on following criteria: molecular weight (MW) < 500, log P < 5, hydrogen bond donor (HBD) <5 and hydrogen bond acceptor (HBA) < 10, Lipinski Rule of five was initially applied to filter compounds. Then Rule of Verber was applied for further screening of compounds to determine the oral bioavailability of drug that contains polar surface area ≤ 140 and number of rotatable bonds (FrRotB) ≤10 [32].

Based on water solubility (mg/mL) ≥ 0.010 and MDCK (Apparent Madin-Darby canine kidney cell permeability) ≥ 30, compounds were further screened to determine aqueous solubility and membrane permeability [40]. To filter out compounds that do not have blood brain barrier permeability (-BBB), then two parameters, Log BB and BBB filter were taken into consideration. Based on two key parameters Log BB and BBB (Blood Brain Barrier) filter, further filtration was performed. Log BB < -1 and BBB filter = low% were applied for BBB- group [41]. Next phase of screening of compounds was performed on the basis of their cardiotoxicity (hERG filter = No, and hERG pIC50 < 5.5) and carcinogenicity (BCRP inhibitor = No) properties.

Ligands preparation

From PubChem database, ligands structures were initially downloaded in 3D SDF format and then subsequently transformed into PDB format by using BIOVIA Discovery Studio Visualizer [33]. With the help of Auto Dock 1.5.7v tools [34][35], PDB format further converted into PDBQ by adding polar hydrogen bonds and Gasteiger charges.

Molecular docking

Using AutoDock vina 1.5.7 [35], molecular docking experiments was conducted. Screened ligands were docked with the target protein VP39 MTase (8cer). From the 96 ligands based on ADMET criteria, top ten ligands with the lowest binding energy was selected. Further analysis of obtained top 10 docked complexes was done by BIOVIA Discovery Studio Visualizer [33]. Where various interactions including hydrogen bonding, van der Waals forces, hydrophobic interaction and alkyl interaction were analyzed to examine their involvement with active site residues. For further visualization, lowest binding energy ligands were selected for DFT and MD simulation.

Density functional theory

To evaluate a ligand's reactivity and compatibility with the target protein, DFT is used. After molecular docking studies, DFT study was performed to assess the reactivity of final selected compounds. To determine the reactivity of compound with the lowest binding energy towards the target protein VP39 MTase (8cer) among the top 10 ranked compounds, DFT was employed before proceeding towards molecular simulation. To determine the energy gap ΔE, LUMO-HOMO expression was used to measure the difference between highest occupied molecular orbital (HOMO) and lowest unoccupied molecular orbital (LUMO) [42]. Using Gaussian 09 [43], DFT analysis was performed. DFT/B3LYP (Density functional theory/Becke 3-parameter Lee-Yang-Parr) together with 6-31 G basis set was applied for optimization of compound [44]. To obtain the findings and visualize the .chk file in recovered file fragment format, Gauss view 6.0 was used.

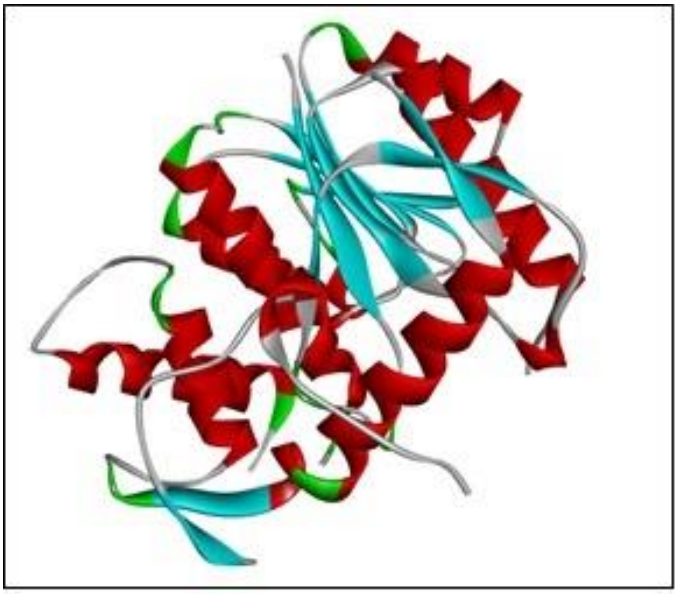

Figure 2. 3D structure of VP39 MTase protein (PDB ID: 8cer, resolution 2.60Å) of MPXV [44]

Results

Structure verification and physiochemical properties

From Protein databank (PDB ID: 8cer), structure of protein VP39 MTase was retrieved and verified with the help of three validation servers: ERRAT [26], Verify 3D [27] and PROCHECK [28]. 94.393 was the overall quality factor of VP39 MTase (8cer) shown by ERRAT analysis. The Ramachandran plot in the PROCHECK showed 93.5% in most favoured regions, 6.5% residues in additional allowed regions and 0.0% residues in disallowed region. Verify 3D analysis showed that 74.91% residues have averaged 3D-1D score > =0.1. Their findings confirmed that structure of protein VP39 Mtase (8cer) is reliable, well-resolved and of good quality is illustrated in Table S1.

Analysis of physiochemical characterization of VP39 MTase (8cer) showed the stability of protein. Their

Table 1. ADMET criteria with their recommended ranges for library preparation for molecular docking

No. of properties	ADMET properties	Recommended ranges
1.	**Lipinski rule of five (ROF)**	
	Mol. Weight (Dalton)	<500 Dalton
	Log P	≤5
	Hydrogen bond donor	≤5
	Hydrogen bond acceptor	≤10
2.	**Rule of Verber**	
	No. of rotatable bond (FrRotB)	<10
	Total polar surface area	<140
3.	Water solubility (Sw)	≥0.010 mg/mL
4.	Apparent Madin-Darby canine kidney cell permeability (MDCK)	≥30 cm/s ×10^7
5.	Log BB	<-1 (for BBB-)
6.	Blood Brain Barrier filter	Low (%) for (BBB-)
7.	BCRP_Inh	No
8.	hERG filter	No
9.	hERG pIC50	<5.5

Table 2. Screened ligands according to ADMET criteria

Sr. No	ADMET criteria selected	Recommended ranges	Ligand screened
1.	Water solubility (Sw)	≥0.010 mg/mL	4899
2.	Apparent Madin-Darby canine kidney Cell permeability (MDCK)	≥30cm/s × 10^7	4078
3.	Log BB	< -1 (for BBB-)	165
4.	Blood Brain Barrier filter	Low (%) for (BBB-)	112
5.	BCRP_Inh	No	102
6.	hERG Filter	No	100
7.	hERG pIC50	<5.5	96

visualization indicates that molecular weight of protein is 38886.98. 9.47 is theoretical Pi of target protein. Aliphatic index of protein is 88.65 indicate their thermostability since high aliphatic index is associated with enhanced thermal stability [45]. For VP39 MTase (8cer), the GRAVY (grand average of hydropath) values were calculated as -0.395, the negative values signifying that protein exhibit non-polar nature [46]. Protein exhibit 30 hours half-life in mammalian reticulocyte cell in-vitro due to methionine as N-terminal residue [45]. These physiochemical properties are illustrated in Table S2.

Screened ligands

Based on ADMET (absorption, distribution, metabolism, excretion and toxicity) criteria, 17967 compounds were screened. 4899 compounds were screened form the library of 17967 compounds after applying Lipinski Rule of five and Verber rule. After applying additional screening criteria, including MDCK permeability, water solubility, BCRP, hERG filter and hERG pIC50, 96 ligands were selected for further analysis. The hERG filter was set to No to prevent the selection of cardiotoxic compounds [47]. Then the active site VP39 MTase (8cer) was targeted for docking with the screened 96 ligands. All 96 compounds could not cross blood brain barrier, leading to their classification in (-BBB) group. Number of screened ligands in all parameters shown below in Table 2.

Docking analysis

Out of 17967 compounds library, 96 screened ligands were docked at the active site of target protein VP39 MTase (8cer) which will inhibit the protein. Docked ligands were sorted based on their lowest binding energies. From the 96 docked complexes, top-10 compounds were selected for further analysis based on their lowest binding energies are listed in Table 3. Binding energy values of these ligands revealed by docking results varied from -7.6kcal/mol to -6.8kcal/mol. Further analyzation of interaction between ligands and receptors was done by using BIOVIA Discovery Studio Visualizer [33]. The PubChem ID,

molecular formula, IUPAC name, 2D structure and types of interaction of top 10 ligands are shown in Table 4.

For VP39 MTase (8cer), one compound with lowest binding energy from 10 top-ranked docked complexes was selected. Compound-1 (Hispidin) with PubChem ID: 54685921 had the lowest binding energy of -7.6kcal/mol. To visualize the results and interaction in the active sites, BIOVIA Discovery Studio Visualizer was used. Compound-1 (Hispidin) bound to the active site of VP39 MTase (8cer) is shown in Fig 3. (A). The ligand exhibited various interaction with VP39 MTase (8cer) receptor, including conventional hydrogen bond interaction with VAL 116 having a distance of 2.81Å, van der Waals interaction with LEU 159, ILE 67, ILE 94, ARG 114, ASP 95, GLY 96, GLY 68, ASP 138, ALA 70 and PRO 71 as shown in Fig 3. (D). Pi-alkyl interaction seen between ARG 140 at a distance angle of 4.51Å, Pi- Sigma form bond with VAL 139 with a distance of 3.87Å, Pi-Pi T-shaped is seen with PHE 115 with aromatic ring of ligand at a distance angle of 4.81Å, Pi-Cation show interaction with ARG 97 between the distance of 4.15Å and 5.30Å respectively as shown in Fig 3. (C).

Table 4. DFT analysis of 10 selected compounds with lowest binding energy of VP39 MTase (8cer) protein

Compound name	LUMO	HOMO	Energy gap (ΔE)
CID_ 54685921	-0.08010	-0.20736	0.12726eV
CID_13370052	-0.01144	-0.22971	0.21827eV
CID_23724664	-0.00715	-0.20083	0.19368eV
CID_14018348	-0.07448	-0.22012	0.14564eV
CID_441777	-0.02310	-0.14650	0.1234eV
CID_13935024	-0.03230	-0.22096	0.18866eV
CID_32281	-0.00587	-0.22752	0.22165eV
CID_99693	-0.07141	-0.23380	0.16239eV
CID_441694	-0.01991	-0.14535	0.12544eV
CID_10095770	-0.06497	-0.21034	0.14537eV

Table 3. 10 compounds with lowest binding energies selected for VP39 MTase protein

Ligands	PubChem ID	2D structure	Molecular formula	Binding energy	Hydrogen bond interaction	Van der waals interaction	Alkyl interaction	Other interactions
1-Hispidin	CID_54685921	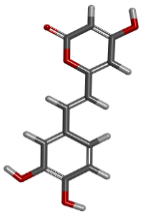	$C_{13}H_{10}O_5$	-7.6	VAL A:116	LEU A:159, ILE A:67 ILE A:94 ASP A:95, ARG A:114, GLY A:96, GLY A:68, ASP A:138, ALA A:70, PRO A:71	ARG A:140	Pi-sigma interaction: VAL A:139 Pi-Pi T shaped interaction: PHE A:115 Pi-cation interaction: ARG A:97

2- 7Beta-Hydroxydehydroabiet-ic Acid	CID_13370052	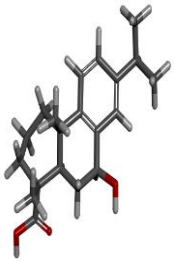	$C_{20}H_{28}O_3$	-7.5	SER A:289	ASP A:80, PHE A:293, ILE A:290, HIS A:81, LEU A:85, ASN A:273, CYS A:272, LYS A:274, PHE A:285,	TYR A:77	Carbon hydrogen bond: ASN A:84
3- Medicarpin 3-O-glucoside	CID_23724664	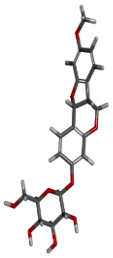	$C_{22}H_{24}O_5$	-7.5	ILE A:94 ARG A:114, VAL A:116, ARG A:140, ARG A:97	ASP A:95, GLY A:96, PHE A:115, GLY A:68, ILE A:67, LEU A:159, VAL A:139, SER A:141, LEU A:42, GLN A:39	PRO A:71	Carbon hydrogen bond interaction: ALA A:70 Unfavourable donor-donor interaction: ASP A:138
4-Boeravinone B	CID_14018348	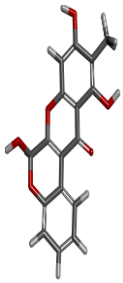	$C_{17}H_{12}O_6$	-7.2	ASN A:84	ARG A:292, PHE A:293, TYR A:77, ASP A:80, HIS A:81 TYR A:271, LEU A:85, ASN A:273, CYS A:272, LYS A:274, PHE A:285		
5-Rosinidin	CID_441777	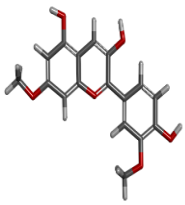	$C_{17}H_{15}O_6^+$	-7.1	TYR A:77 HIS A:81	LEU A:85, ASP A:80, PHE A:293, ASN A:273, LYS A:274, PHE A:285	ARG A:292	Carbon hydrogen bond interaction: ASN A:84, SER A:289

6- cis-Zeatin riboside	CID_13935024	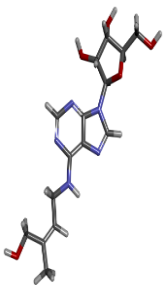	$C_{15}H_{21}N_5O_5$	-7.1	HIS A:81	LEU A:286, CYS A:272, ASP A:80, ARG A:76, LEU A:85, PHE A:285, ASN A:84, ARG A:292		Pi-donor hydrogen bond interaction: TYR A:77, PHE A:293, SER A:289 Unfavourable donor-donor interaction: LYS A:274, ASN A:273
7-Protirelina	CID_32281	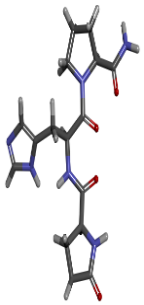	$C_{16}H_{22}N_6O_4$	-6.9	ASP A:138 GLY A:68	ILE A:75 SER A:69, TYR A:66, HIS A:74, GLY A:72, GLN A:39, LYS A:41, GLY A:38, ARG A:97, VAL A:139, ASP A:95, GLY A:96, PHE A:115, LYS A:175	LEU A:42, PRO A:71	Carbon hydrogen bond interaction: ALA A:70 Unfavourable donor-donor interaction: ARG A:140
8-Skimmin	CID_99693	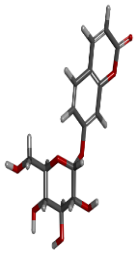	$C_{15}H_{16}O_8$	-6.8	ASN A:273,	LEU A:85, ASN A:84, ASP A:80, PHE A:293, ARG A:292, SER A:289, PHE A:285, CYS A:272		Unfavourable donor donor interaction : HIS A:81, LYS A:274 Pi-Pi stacked interaction: TYR A:77
9-Hirustidin	CID_441694	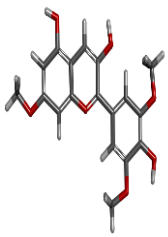	$C_{18}H_{17}O_7^+$	-6.8		ASP A:80, PHE A:293, PHE A:285, LYS A:274, CYS A:272	ARG A:292	Carbon hydrogen bond interaction: SER A:289, ASN A:84 Pi-Pi stacked interaction: TYR A:77 Unfavourable donor-donor interaction: HIS A:81

10- Wistin	CID_10095770	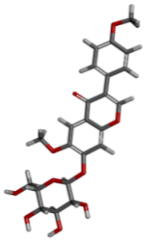	$C_{23}H_{24}O_{10}$	-6.8	TYR A:66 GLY A:68	VAL A:139, ARG A:140, ARG A:97, GLN A:39, SER A:69, LEU A:42, PRO A:71, GLY A:72, HIS A:74, GLY A:38, LYS A:41, GLN A:37, SER A:203	PRO A:202	Carbon hydrogen bond interaction: ASP A:138, ALA A:70

Discussion

Monkeypox is a contagious zoonotic disease belong to Poxviridae family. In Democratic Republic of Congo in 1970, the first human case of monkeypox was recorded [50]. When monkeys were transferred from Singapore to Denmark for polio vaccine research to an animal facility, MPXV was first detected in Asian monkeys in 1958. The virus was first time observed in monkeys, that's why it was named as MPXV [51]. MPXV mainly seen in Central and West African countries but has spread to various other countries both in and outside of Africa [52]. WHO declared the Public Health Emergency of International Concern (PHEIC) on 23 July 2022 due to ongoing global monkeypox outbreak [53].

Fever, severe headache, myalgia, fatigue are initial clinical symptoms of MPXV. Within 1-3days of onset of fever, skin lesion begins to appear [50]. Most patients during 2022 outbreak developed fever, rash with papules progressing to crusts, vesicles in the oral, anal or genital regions and the incubation period ranged from 7-10 days [54]. It can be transmitted via mucosal exposure and direct skin contact to infected animals [55]. Most cases have been diagnosed among men who have sex with men and 2022 outbreak has been associated with close intimate contact [54].

No drug has been specifically designed for the prevention and treatment of MPXV [12]. Attention must be needed towards it before it causes the next epidemic after the SARS-CoV-19. Unfortunately, drug development by traditional de novo technique takes years to produce clinical results. Alternately, modern techniques for drug designing such as drug repurposing may help to provide more rapid solutions [15].

To find the antiviral agents against MPXV, this study was designed. VP39 MTase was chosen as a target due to its role in viral replication and immune evasion. Viral enzyme can be considered as a promising target for treatment because of its role in DNA synthesis, transcription and modification of viral proteins. VP39 MTase modifies mRNA to enhance protein synthesis and escape host immunity [23].

Our study aimed to identify potential inhibitor for this enzyme using docking and DFT based on the importance of VP39 MTase in viral infection within the host [24]. From the protein databank, the crystal structure of VP39 MTase (PDB ID: 8cer) was selected because of having greater sequence coverage. By using *SAVES* v6.1, structure validation of protein was done and physiochemical properties were checked from ExPASY PortParam tool.

In this study, we used a strategy to find 17967 compounds from the Indian Medicinal plant database, the IMPPAT library [56]. On the base of Lipinski Rule of five (ROF) and ADMET criteria, 96 ligands screened out of 17967 compounds. The PDB structure of target was retrieved from PDB ID: 8cer and prepared for molecular docking with 96 screened ligands fulfilling ADMET criteria. Screened ligands were docked against the active site of VP39 MTase (8cer). Top ten docked ligands were selected based on their lowest binding energies ranging from -7.6kcal/mol to -6.8kcal/mol. Only one compound (PubChem ID: 54685921) from top ten ligands was selected with lowest binding energy of -7.6kcal/mol for further visualization.

To check the kinetic stability and chemical reactivity of the ligands, lowest binding energy compounds were further analyzed for DFT analysis. 0.12726eV is the energy gap ΔE of compound-1 (Hispidin). The compound is reactive towards our target VP39 MTase (8cer) because of lower energy gap. To check the reactivity of compound, DFT analysis was done. By MD simulation, further validation

was provided. In future research, further MD simulation will be employed to confirm our current results.

Conclusions

In drug discovery, the computational analysis is rapid and effective technique and can found the potential inhibitor in less time as it does not require funding. VP39 MTase (8cer) was selected as receptor against MPXV. To find the potential inhibitor, computational analysis was performed for it. In our study, we concluded that the compound-1 Hispidin (PubChem ID:54685921) showing the lowest binding energy through molecular docking and DFT. Result shows that the compound-1 is a potential inhibitor for VP39 MTase (8cer). In future research, further MD simulation will be employed to confirm our current results but more in vivo and in vitro testing is needed to confirm antagonistic suggested in this work.

Authors' contributions

ICMJE criteria	Details	Author(s)
1. Substantial contributions	Conception, OR Design of the work, OR Data acquisition, analysis, or interpretation	1 2 3
2. Drafting or reviewing	Draft the work, OR Review critically for important intellectual content	1,2 3
3. Final approval	Approve the version to be published	1,2,3
4. Accountable	Agree to be accountable for all aspects of the work	1,2,3

Acknowledgement

None

Funding

This research study received no specific grant from any funding agency.

Availability of data and materials

The datasets used and/or analyzed during the current study are available from the corresponding author on reasonable request.

Declarations

Ethics approval and consent to participate

The Ethics Review Committee of University of Management and Technology, Lahore approved the study.

Consent for publication

Not applicable.

Competing interests

The authors declare no competing interests.

Supplementary material

Available from: https://drive.google.com/file/d/1btFni8W1v-7eB8SmhF-GWYxkSxjcD0_F/view?usp=drive_link

References

[1]. Ferdous J, Barek MA, Hossen MS, Bhowmik KK, Islam MS. A review on monkeypox virus outbreak: New challenge for world. Health Sci Rep. 2023;6(1):e1007.

[2]. Ghaseminia M. Preventing monkeypox outbreaks: Focus on diagnosis, care, treatment, and vaccination. J Clin Translat Sci. 2023;7(1):e60.

[3]. de la Calle-Prieto F, Estébanez Muñoz M, Ramírez G, Díaz-Menéndez M, Velasco M, Azkune Galparsoro H, et al. Treatment and prevention of monkeypox. Treatment and prevention of monkeypox. Enfermedades infecciosas y microbiologia clinica (English ed.). 2023;41(10):629-34.

[4]. Khani E, Afsharirad B, Entezari-Maleki T. Monkeypox treatment: Current evidence and future perspectives. J Med Virol. 2023;95(1):e28229.

[5]. Gupta AK, Talukder M, Rosen T, Piguet V. Differential Diagnosis, Prevention, and Treatment of mpox (Monkeypox): A Review for Dermatologists. Am J Clin Dermatol. 2023 Jul;24(4):541-56.

[6]. de la Calle-Prieto F, Estébanez Muñoz M, Ramírez G, Díaz-Menéndez M, Velasco M, Azkune Galparsoro H, et al. Treatment and prevention of monkeypox. Treatment and prevention of monkeypox. Enfermedades infecciosas y microbiologia clinica (English ed.). 2023;41(10):629-34.

[7]. Goyal L, Ajmera K, Pandit R, Pandit T. Prevention and Treatment of Monkeypox: A Step-by-Step Guide for Healthcare Professionals and General Population. Cureus. 2022;14(8): DOI: 10.7759/cureus.28230.

[8]. Patel M, Adnan M, Aldarhami A, Bazaid AS, Saeedi NH, Alkayyal AA, et al. Current Insights into Diagnosis, Prevention Strategies, Treatment, Therapeutic Targets, and Challenges of Monkeypox (Mpox) Infections in Human Populations. Life. 2023;13(1):249.

[9]. Shuvo PA, Roy A, Dhawan M, Chopra H, Emran T Bin. Recent outbreak of monkeypox: Overview of signs, symptoms, preventive measures, and guideline for supportive management. Int J Surg. 2022;105:106877.

[10]. Hossain FMA, Bappy MNI, Robin TB, Ahmad I, Patel H, Jahan N, et al. A review on computational studies and bioin-

formatics analysis of potential drugs against monkeypox virus. J Biomol Struct Dyn. 2024;42(12):6091–107.
[11]. Bajrai LH, Alharbi AS, El-Day MM, Bafaraj AG, Dwivedi VD, Azhar EI. Identification of Antiviral Compounds against Monkeypox Virus Profilin-like Protein A42R from Plantago lanceolata. Molecules. 2022 N;27(22).
[12]. Naveed M, Shabbir MA, Ain NU, Javed K, Mahmood S, Aziz T, et al. Chain-Engineering-Based De Novo Drug Design against MPXVgp169 Virulent Protein of Monkeypox Virus: A Molecular Modification Approach. Bioengineering. 2023 ;10(1):11.
[13]. Mohapatra RK, Mahal A, Mohapatra PK, Sarangi AK, Mishra S, Alsuwat MA, et al. Structure-based discovery of F. religiosa phytochemicals as potential inhibitors against Monkeypox (mpox) viral protein. J Biosaf Biosecur. 2024;6(3):157–69.
[14]. Pastula DM, Tyler KL. An Overview of Monkeypox Virus and Its Neuroinvasive Potential. Ann Neurol. 2022;92(4):527-31.
[15]. Ali Y, Imtiaz H, Tahir MM, Gul F, Saddozai UAK, ur Rehman A, et al. Fragment-Based Approaches Identified Tecovirimat-Competitive Novel Drug Candidate for Targeting the F13 Protein of the Monkeypox Virus. Viruses. 2023;15(2):570.
[16]. Hraib M, Jouni S, Albitar MM, Alaidi S, Alshehabi Z. The outbreak of monkeypox 2022: An overview. Ann Med Surg. 2022;79:104069.
[17]. Hatmal MM, Al-Hatamleh MAI, Olaimat AN, Ahmad S, Hasan H, Ahmad Suhaimi NA, et al. Comprehensive literature review of monkeypox. Emerg Microb Infect. 2022;11(1):2600-31.
[18]. Bajrai LH, Alharbi AS, El-Day MM, Bafaraj AG, Dwivedi VD, Azhar EI. Identification of Antiviral Compounds against Monkeypox Virus Profilin-like Protein A42R from Plantago lanceolata. Molecules. 2022;27(22):7718.
[19]. Abouzied AS, Huwaimel B, Alqarni S, Younes KM, Alshammari RE, Alshammari AH, et al. Sinefungin analogs targeting VP39 methyltransferase as potential anti-monkeypox therapeutics: a multi-step computational approach. Mol Divers. 2025;29(1):561-74.
[20]. Thai QM, Phung HTT, Pham NQA, Horng JT, Tran PT, Tung NT, et al. Natural compounds inhibit Monkeypox virus methyltransferase VP39 in silico studies. J Biomol Struct Dyn. 2024; https://doi.org/10.1080/07391102.2024.2321509.
[21]. Subramaniam D, Thombre R, Dhar A, Anant S. DNA methyltransferases: A novel target for prevention and therapy. Front Oncol.2014; https://doi.org/10.3389/fonc.2014.00080.
[22]. Hodel AE, Gershon PD, Shi X. The 1.85 A ˚ Structure of Vaccinia Protein VP39: A Bifunctional Enzyme That Participates in the Modification of Both mRNA Ends. Cell. 1996;85(2):247-56.
[23]. Hassan AM, Gattan HS, Faizo AA, Alruhaili MH, Alharbi AS, Bajrai LH, et al. Evaluating the Binding Potential and Stability of Drug-like Compounds with the Monkeypox Virus VP39 Protein Using Molecular Dynamics Simulations and Free Energy Analysis. Pharmaceuticals. 2024;17(12):1617.
[24]. Hashim HO, Al-Shuhaib JMB, Mohammed MK, Al-Shuhaib MBS. Targeting Monkeypox Virus Methyltransferase: Virtual Screening of Natural Compounds from Middle-Eastern Medicinal Plants. Mol Biotechnol. 2024; https://doi.org/10.1007/s12033-024-01246-y.
[25]. Vivek-Ananth RP, Mohanraj K, Sahoo AK, Samal A. IMPPAT 2.0: An Enhanced and Expanded Phytochemical Atlas of Indian Medicinal Plants. ACS Omega. 2023;8(9):8827–45.
[26]. Colovos C, Yeates TO. Verification of protein structures: Patterns of nonbonded atomic interactions. Protein Sci. 1993;2(9):1511–9.
[27]. Verify3D – UCLA-DOE Institute [Internet]. Available from: https://www.doe-mbi.ucla.edu/verify3d/
[28]. Laskowski RA, MacArthur MW, Moss DS, Thornton JM. PROCHECK: a program to check the stereochemical quality of protein structures. J Appl Crystallogr. 1993;26(2):283–91.
[29]. Bhattacharjee A, Ahammad I, Chowdhury ZM, Das KC, Keya CA, Salimullah M. Proteome-Based Investigation Identified Potential Drug Repurposable Small Molecules Against Monkeypox Disease. Mol Biotechnol. 2024;66(4):626–40.
[30]. Raen R, Islam MM, Islam R, Islam MR, Jarin T. Functional characterization and structural prediction of hypothetical proteins in monkeypox virus and identification of potential inhibitors. Mol Divers. 2024; 70(8):39-49.
[31]. Hosen MI, Mia ME, Islam MN, Khatun MUS, Emon TH, Hossain MA, et al. In-silico approach to characterize the structure and function of a hypothetical protein of Monkeypox virus exploring Chordopox-A20R domain-containing protein activity. Antivir Ther. 2024;29(3).
[32]. Adrees S, Imtiaz A, Yaseen A, Irfan Fareed M, Anwar W, Ashraf A, et al. In-silico analysis of potential anticancer drug for NEK7 and PPP1CA proteins overexpressed in pancreatic ductal adenocarcinoma. J Biomol Struct Dyn. 2024; https://doi.org/10.1080/07391102.2024.2318484.
[33]. Shaweta S, Akhil S, Utsav G. Molecular Docking studies on the Anti-fungal activity of Allium sativum (Garlic) against Mucormycosis (black fungus) by BIOVIA discovery studio

visualizer 21.1.0.0. Annals of Antivirals and Antiretrovirals. 2021; 5(1):028-32.

[34]. Eberhardt J, Santos-Martins D, Tillack AF, Forli S. AutoDock Vina 1.2.0: New Docking Methods, Expanded Force Field, and Python Bindings. J Chem Inf Model. 2021;61(8):3891–8.

[35]. Trott O, Olson AJ. AutoDock Vina: Improving the speed and accuracy of docking with a new scoring function, efficient optimization, and multithreading. J Comput Chem. 2010;31(2):455–61.

[36]. Wu Q, Peng Z, Zhang Y, Yang J. COACH-D: Improved protein-ligand binding sites prediction with refined ligand-binding poses through molecular docking. Nucleic Acids Res. 2018;46(W1):W438–42.

[37]. Jendele L, Krivak R, Skoda P, Novotny M, Hoksza D. PrankWeb: a web server for ligand binding site prediction and visualization. Nucleic Acids Res. 2019 ;47(W1):W345–9.

[38]. Sharma A, Roy S, Parijat Tripathi K, Roy P, Mishra M, Khan F, et al. Predicted metal binding sites for phytoremediation. Bioinformation [Internet]. 2009;4(2):66–70. Available from: http://www.cprm.gov.br/pgagem/Manuscripts/jeliazkovaea.ht

[39]. Benet LZ, Hosey CM, Ursu O, Oprea TI. BDDCS, the Rule of 5 and drugability. Vol. 101, Adv Drug Delivery Rev. 2016;101:89-98.

[40]. Irvine JD, Takahashi L, Lockhart K, Cheong J, Tolan JW, Selick HE, et al. MDCK (Madin-Darby canine kidney) cells: A tool for membrane permeability screening. J Pharm Sci. 1999;88(1):28–33.

[41]. Kunwittaya S, Nantasenamat C, Treeratanapiboon L, Srisarin A, Isarankura-Na-Ayudhya C, Prachayasittikul V. Influence of logBB cut-off on the prediction of blood-brain barrier permeability. Biomed Applied Technol J. 2013;1:16-34.

[42]. Bredas JL. Mind the gap! Mater Horiz. 2014;1(1):17-9.

[43]. Frisch A. gaussian 09W Reference. Wallingford, USA, 25p. 2009;470.

[44]. Dagli M, Er M, Karakurt T, Onaran A, Alici H, Tahtaci H. Synthesis, Characterization, Antimicrobial Evaluation, and Computational Investigation of Substituted Imidazo [2, 1-b][1, 3, 4] thiadiazole Derivatives. Chemistry Select. 2020;5(38):11753-63.

[45]. Ikai A. Thermostability and Aliphatic Index of Globular Proteins. J Biochem. 1980;88(6):1895-8.

[46]. Kyte J, Doolittle RF. A Simple Method for Displaying the Hydropathic Character of a Protein. J Mol Biol. 1982;157(1):105-32.

[47]. Plaster NM, Tawil R, Tristani-Firouzi M, Canú S, Saı¨d Bendahhou S, Tsunoda A, et al. Mutations in Kir2.1 Cause the Developmental and Episodic Electrical Phenotypes of Andersen's Syndrome 17q23 (maximum LOD 3.23 at 0) near the inward rectifying potassium channel gene KCNJ2. A missense Frank A. Fish, 12 Angelika Hahn, 13 Alexandru Nitu, 14 Coskun Ozdemir, 11 Piraye Serdaroglu, 11 mutation in KCNJ2 (encoding D71V) was identified in the linked family. Cell. 2001;105(4):511-9.

[48]. Sib Tul Hassan Shah S, Naeem I. In-silico targeting TMPK from monkey pox virus: Molecular docking analysis, density functional theory studies and molecular dynamic simulation analysis. J Biomol Struct Dyn. 2023;41(24):14689–701.

[49]. Naeem I, Mateen RM, Sibtul Hassan S, Tariq A, Parveen R, Saqib MAN, et al. In silico identification of potential drug-like molecules against G glycoprotein of Nipah virus by molecular docking, DFT studies, and molecular dynamic simulation. J Biomol Struct Dyn. 2023;41(15):7104–18.

[50]. Kaswa R, Nair A, Von Pressentin KB. South African Family Practice. 2022; Available from: https://doi.org/10.4102/safp.

[51]. Rampogu S, Kim Y, Kim SW, Lee KW. An overview on monkeypox virus: Pathogenesis, transmission, host interaction and therapeutics. Front Cellular Infect Microbiol. 2023;13:1076251.

[52]. Yadav AK, Srivastava A, Verma P, Gupta D. A Comprehensive Review on Monkeypox Virus Transmission, Pathogenesis, Treatments and its Preventive Measures. Available from: https://www.researchgate.net/publication/365472703

[53]. Saied ARA, Dhawan M, Metwally AA, Fahrni ML, Choudhary P, Choudhary OP. Disease History, Pathogenesis, Diagnostics, and Therapeutics for Human Monkeypox Disease: A Comprehensive Review. Vaccines. 2022;10(12):2091.

[54]. Mitjà O, Ogoina D, Titanji BK, Galvan C, Muyembe JJ, Marks M, et al. Monkeypox. Lancet. 2023;401(10370):60-74.

[55]. Zahmatyar M, Fazlollahi A, Motamedi A, Zolfi M, Seyedi F, Nejadghaderi SA, et al. Human monkeypox: history, presentations, transmission, epidemiology, diagnosis, treatment, and prevention. Front Med. 2023;10:1157670.

[56]. Vivek-Ananth RP, Mohanraj K, Sahoo AK, Samal A. IMPPAT 2.0: An Enhanced and Expanded Phytochemical Atlas of Indian Medicinal Plants. ACS Omega. 2023;8(9):8827–45.